ELSEVIER

Colloids and Surfaces
A: Physicochemical and Engineering Aspects 134 (1998) 331–342

COLLOIDS AND SURFACES A

Modification of ultrafiltration membranes by deposition of colloid particles

R.G. Alargova, J.T. Petkov, N.D. Denkov *, D.N. Petsev, I.B. Ivanov

Laboratory of Thermodynamics and Physico-Chemical Hydrodynamics, Faculty of Chemistry, University of Sofia, Sofia 1126, Bulgaria

Received 3 March 1997; accepted 4 August 1997

Abstract

We describe an experimental procedure for the modification of ultrafiltration membranes by the deposition of monodisperse polymer spheres. The conditions for irreversible formation of particulate deposit are studied and correlated with the particle charge. The separation characteristics of the membranes before and after particle deposition are compared. For this purpose, a method for determining the membrane rejection coefficient is developed. The method is based on the light-scattering study of permeates obtained upon the filtration of commercial dextran samples. The results show that the modified membranes have improved retention characteristics. © 1998 Elsevier Science B.V.

Keywords: Dynamic light scattering from dextran solutions; Membrane characterization; Membrane modification; Retention coefficient of membranes

1. Introduction

Membrane pore size distribution is an important characteristic determining the application and performance of a membrane in filtration processes [1,2]. The mean pore size characterizes the typical size range of particles that can be separated. More narrow pore size distribution corresponds to a better selectivity of the membrane.

One possibility for preparing a membrane with a required pore size and a relatively narrow size distribution could be the coating of the membrane surface with more- or less-ordered layers of monodisperse particles. For instance, when a colloidal suspension is filtered through a membrane, an accumulation of particles in the vicinity of the membrane surface takes place (cake formation) [2,3]. When the particles are spherical and monodisperse, this filter cake may consist of well ordered multilayered array — see, for example, Fig. 1.6 in Ref. [3]. If the suspension is very stable, the filter cake destructs spontaneously after the filtration is ceased. At certain conditions, however, the particles in the layer coagulate, forming a structure which cannot redisperse in the suspension [3]. This problem of colloidal stability was examined from a theoretical viewpoint and quantitative criteria for the formation of irreversibly coagulated layer were formulated [4]. With respect to the filtration process, such a layer presents a second membrane with a given mean pore size and a relatively narrow pore size distribution. Only solutes with radius, R, smaller than a given cut-size (which is determined by the diameter and the spatial arrangement of the deposited particles) could pass through the membrane. For example, in the case of a perfect

* Corresponding author.

PII S0927-7757(97)00221-5

hexagonal packing of monodisperse spheres of radius a, one can estimate:

$$R \leqslant a\left(\frac{2\sqrt{3}}{3}-1\right) \approx 0.155a. \quad (1)$$

Thus, one may expect that an ordered multilayer from particles of, for example, radius 50 nm, should correspond to a membrane with a rather narrow pore size distribution centered around 8 nm.

The molecular weight cut-off (MWCO) value and the partial rejection coefficient are usually used as main characteristics of the membrane retention ability [1,2]. These quantities can be determined by filtration of reference polymer solutes (e.g. proteins, polyoxyethylenes or dextrans) of known molecular mass at standard conditions. From the concentrations of the polymer of mass M before and after filtration, the partial rejection coefficient, $Re(M)$, can be obtained [2]:

$$Re(M)\% = \left(1 - \frac{C_p(M)}{C_f(M)}\right) \times 100, \quad (2)$$

where $C_p(M)$ and $C_f(M)$ are the polymer concentrations in the permeate and the feed solution, respectively. MWCO is usually defined as the molecular mass of a polymer, which is 90% rejected by the membrane [5,6], i.e. $Re(\mathrm{MWCO}) = 90\%$.

Different experimental procedures for determination of the MWCO have been proposed in the literature [5–7]. Some authors recommend the use of a feed solution containing a polymer mixture with a wide molecular mass distribution [6,7]. This procedure allows determination of the $Re(M)$ and MWCO of a given membrane by performing only one ultrafiltration experiment. However, this method has an important disadvantage: when a mixture of polymer molecules with rather different sizes are filtered, the larger molecules may form a dynamic membrane thus apparently increasing the rejection of smaller molecules. For this reason, other authors argue that the polymer samples of different mass must be tested separately [5]. The feed solutions and the permeates in such experiments are usually analyzed by gel permeation chromatography in order to obtain the molecular mass distributions and to calculate $Re(M)$ [6,7]. However, the gel permeation chromatography requires a precise calibration using polymer standards with *very narrow* molecular mass distribution. These standards are rather expensive and not readily available [6,8].

In the present work, we describe experiments on membrane modification by filtration of monodisperse latex particles, which form a deposit (particle multilayer) at the membrane surface. The permeability and the retention characteristics of the membranes, before and after their modification, are compared. The partial rejection coefficients and MWCO are determined by filtration of commercial (polydisperse) dextran solutions, which are studied by dynamic light scattering before and after passing through the membrane. The effect of the particle charge on the formation of the deposited particle layer is studied. The results show that at relatively "soft conditions" (low driving pressure), irreversibly deposited particulate layers can be obtained from particles possessing a ζ potential of a magnitude below approximately 30 mV. The modification of the membranes leads to lower MWCO and improved selectivity.

2. Experimental

2.1. Materials

We used polysulphonic ultrafiltration membranes produced by DOW Separations, Denmark (named MWCO 20 kD) and the Insitute of Chemical Technology, Plovdiv, Bulgaria (MWCO 150 kD). The membranes were treated by several types of particles. Two samples of polystyrene latex were kindly supplied by Professor Furusawa (University of Tsukuba, Japan). The mean particle diameter of these samples was $d_p = 260$ and 140 nm, respectively. The particles of diameter 140 nm possessed a ζ potential equal to -60 mV, while the particles in the other sample (260 nm) were amphoteric and their ζ potential was strongly pH dependent. Two samples of polybutylcyanoacrylate (PBCA) particles (both of mean diameter $d_p = 107$ nm) were synthesized at the Institute of

Special Polymers (Sofia, Bulgaria). These two samples differed in their ζ potentials: -33 and -12 mV, respectively.

The electrophoretic mobility of the particles was measured by means of Zetasizer IIC equipment (Malvern Instruments, UK) in 0.001 M NaCl. The particle ζ potential was calculated by using the Smoluchowski equation (see, for example, chapter 7 in Ref. [3]). For membrane characterization, we used commercial dextran fractions (Sigma Co. USA) with a molecular mass between 10 and 500 kD — see Table 1. All solutions were prepared with deionized water obtained from a Milli RO4/Milli Q Organex system (Millipore USA).

2.2. Membrane modification by particle deposition

All filtration experiments were performed at room temperature (25 ± 1°C) in a 100 ml ultrafiltration experimental cell produced by the Institute of Chemical Technology, Plovdiv, Bulgaria. It operates in the dead-end mode of filtration and allows continuous stirring to suppress the concentration polarization at the membrane surface. This is particularly important in the experiments aimed to determine the MWCO of the membrane. The transmembrane pressure was created by nitrogen gas and was kept constant (0.5, 1 or 2 bar) during the experiment.

Two series of experiments were performed to study the process of particle deposition. The first set was aimed to show how the thickness of the deposited layer depends on the particle charge. For this purpose, we used the amphoteric latex ($d_p=260$ nm) whose charge was pH dependent. The pH of the suspension was varied by a phosphate buffer, always keeping the ionic strength at 0.001 M. The particle volume fraction in the initial suspension was $\phi=0.1\%$. The filtration experiments were performed with a polysulphonic membrane (MWCO = 150 kD) at a driving pressure of 1 bar. The filtration process was carried out until half of the solution, put in the experimental cell at the beginning, passed trough the membrane.

It has been shown theoretically [4] that the filter cake formed in the course of filtration may consist of two parts: (1) coagulated with permeability K_f^c; and (2) noncoagulated part with permeability K_f^{nc}. These quantities are related to the total permeability, K, the permeability of the clean membrane, K_0, and the transmembrane solvent flux, J_w, by the following expressions:

$$\frac{1}{K}=\frac{1}{K_0}+\frac{1}{K_f^c}+\frac{1}{K_f^{nc}};\ J_w=K\Delta P, \tag{3}$$

where ΔP is the pressure drop across the membrane. The main difference between the coagulated and the noncoagulated parts of the filter cake is that the former remains stable after the end of the filtration process due to strong van der Waals attraction between the particles. The noncoagulated layer is present only during the transmembrane solvent transfer and disappears with the removal of the pressure drop because of the particles' Brownian motion.

The values of K_0, K_f^c and K_f^{nc} can be estimated in the following way:

Table 1
Properties of the studied dextran fractions (Sigma Co.). $\bar{M}$ was measured by static light scattering, whereas $\bar{D}$, R_h and the relative standard deviations $\langle\sigma_M^2\rangle$ and were determined from the size-distribution histograms measured by dynamic light scattering (see Section 2.3 and Appendix A)

Sample	$\bar{M}$ (kD)	$\langle\sigma_M^2\rangle^{1/2}$	$\bar{D}\times10^6$ cm^2 s^{-1}	$\langle\sigma_D^2\rangle^{1/2}$	R_h (nm)
D-9260	9.4	0.420	1.08	0.240	2.35
D-4626	19.6	0.505	0.890	0.243	2.8
D-4133	40.6	0.443	0.548	0.210	4.7
D-1390	71.2	0.459	0.370	0.187	6.0
D-3759	71.5	0.775	0.438	0.229	6.5
D-4876	124	0.348	0.320	0.203	8.0
D-7265	266	0.579	0.192	0.248	12.1
D-5251	510	0.606	0.134	0.277	17.4

(1) First, the permeability of the clean membrane K_0 is determined by measuring the dependence of J_w versus ΔP. The liquid passing through the membrane in this measurement must be identical with the medium in which the latex particles are dispersed.
(2) Then a suspension of latex particles is filtered and the contributions of K_0, K_f^c and K_f^{nc} are measured together (cf. Eq. (3).
(3) After ceasing the filtration, the noncoagulated part of the cake is removed by gentle rinsing of the membrane with pure water and, afterwards, the permeability of the membrane together with the coagulated layer is measured.
(4) From the difference in the permeability measured in steps 2 and 3, one can determine the values of K_f^c and K_f^{nc} separately.

Finally, one can estimate the thickness, L, of the coagulated part built on the membrane surface using the Kozeny–Carman equation [9]:

$$L=\frac{d_p^2(1-\phi_L)^3}{180\eta\phi_L^2K_f^c}, \quad (4)$$

where ϕ_L is the particle volume fraction in the deposited layer (in our calculations, we adopted the value corresponding to closely packed spheres — $\phi_L=0.74$).

The aim of the second series of particle deposition experiments was to investigate how the partial rejection coefficient and the MWCO of a given membrane are affected by the presence of a deposited layer. The particle deposition was performed at 2 bar transmembrane pressure and continuous stirring until half of the fluid in the cell passed through the membrane. The higher pressure in these experiments facilitated the coagulation of the particles on the membrane surface [4]. The modified membranes were gently washed with deionized water (obtained from a Milli RO/Milli Q System) and the characterization procedure as described in Section 2.4 was carried out to determine their rejection coefficient and MWCO.

2.3. Determination of the molecular mass distribution in dextran solutions by light scattering

The light scattering experiments were performed on Malvern 4700C system (Malvern Instruments, UK) equipped with an argon laser Innova 70 (Coherent) operating at a 488 nm wavelength. The temperature of the samples was 25 ± 0.1°C. NaN_3 (0.1 wt.%) was added into the dextran solutions to prevent the growth of bacteria. The ionic strength of the solutions created by NaN_3 was 16 mM. No buffer was used and pH of the solutions was about 6 (±0.5) due to CO_2 dissolved from the air.

The Malvern 4700C system allows one to perform static (SLS) and dynamic (DLS) light-scattering experiments. By SLS, one can determine the average molecular mass of the polymer, $\bar{M}$, and the second osmotic virial coefficient, A_2 (which is related to the intermolecular interactions) [10]:

$$\frac{KC_t}{R_\theta}=\frac{1}{\bar{M}}\left(1+\frac{16\pi n_0^2}{3\lambda^2}R_G^2\sin^2\frac{\theta}{2}\right)+2A_2C_t. \quad (5)$$

Here K is known optical constant; C_t is the total mass concentration of the polymer; R_θ is the Rayleigh ratio determined from the intensity of the scattered light at a given concentration and scattering angle θ; R_G is the radius of gyration of the polymer molecules; n_0 is the solvent refractive index; and λ is the light wavelength in vacuo. Since the studied dextran molecules were relatively small in size, the angular dependence of the scattered light was very weak and R_G could not be determined with reasonable accuracy.

DLS provides information about the *relative concentration* of particles having different diffusion coefficients, $C(D)/C_t$ (i.e. the *diffusion coefficient distribution* of the particles) [11]. The *molecular mass distribution*, $Y(M)=C(M)/C_t$, can be calculated from the diffusion coefficient distribution by using the following relationship [11,12]:

$$M=aD^b \text{ or } \ln M=\ln a=b\ln D, \quad (6)$$

where a and b are constants for a certain homologous series and depend on the type of the polymer, the solvent and the temperature. The constants a and b can be determined experimentally by using several solutions containing polymer of different molecular mass. The intercept and the slope of the linear dependence ln M versus ln D give a and b, respectively. Usually such a calibration line is constructed by using strictly monodisperse samples

(standard deviation in the molecular mass less than approximately 1%). As mentioned above, such samples are rather expensive [6,8]. For this reason, we developed a simple computational procedure which allows the determination of a and b from experiments with polydisperse commercial samples — see the Appendix A.

As an estimate of the size of a polymer molecule of given mass, M, one can use the Stokes–Einstein relationship [13]:

$$R_h(M) = \frac{k_B T}{6\pi\eta D(M)}, \quad (7)$$

where $k_B T$ is the thermal energy, η is the solvent shear viscosity and R_h is the hydrodynamic radius of the polymer molecule.

To check the effect of the polymer concentration on the DLS data, measurements with dextran solutions of different concentrations (between 0.1 and 1 wt.%) were performed. No concentration dependence of the measured mean diffusion coefficient was detected.

2.4. Determination of the rejection coefficient of the membranes

For characterization of the ultrafiltration membranes we used the following experimental procedure.

2.4.1. Filtration of dextran solutions

The filtration experiments were carried out in a batch-stirred filtration cell in dead-end mode. Initially, the influence of the dextran concentration and of the applied transmembrane pressure on the rejection coefficient was checked (see Section 3.2). As a result of these experiments, a dextran concentration of 0.5 wt.% and a pressure of 1 bar were chosen for determination of the partial rejection coefficient of the membranes. We separately filtered several dextran fractions of molecular mass around the expected MWCO value of the investigated membrane. Before each experiment, the ultrafiltration membranes were rinsed with deionized water at 1 bar transmembrane pressure until a constant permeate flux was reached.

2.4.2. Determination of the total dextran concentration and of the molecular mass distribution in the permeate

The total dextran concentration, C_t, was determined by measuring the refractive index of the permeate, n_p, with a sensitive Pulfrich refractometer (Carl-Zeiss, Germany). C_t is proportional to the increase of the refractive index of the solution with respect to that of pure water, n_w:

$$C_t = k(n_p - n_w). \quad (8)$$

The constant $k = 7.14 \pm 0.05$ g/cm^3 was determined experimentally and turned out to be independent (in the framework of the experimental accuracy) on the molecular mass of the dextran used.

On the other hand, DLS gives us the relative molecular mass distribution, $Y(M)$, of the polymer molecules in the solution. The concentration of the polymer molecules, $C(M)$, of a given molecular mass, M, is equal to the product:

$$C(M) = C_t Y(M). \quad (9)$$

The partial rejection coefficient, $Re(M)$, is determined from the change in the concentration $C(M)$ for a number of values of M upon filtration [see Eq. (2)]. The molecular mass corresponding to $Re = 90\%$ is considered as the MWCO value of the ultrafiltration membrane.

3. Results and discussions

Before discussing the results on the membrane modification, we present some data about the properties of the dextran molecules.

3.1. Dextran characterization by light scattering methods

In Fig. 1, the diffusion coefficient of the dextran molecules (as measured by DLS) and the calculated hydrodynamic radius [see Eq. (7)] are presented as functions of the molecular mass. One can see that the diffusion coefficient decreases and the hydrodynamic radius increases with the molecular mass. The curves are well described by the

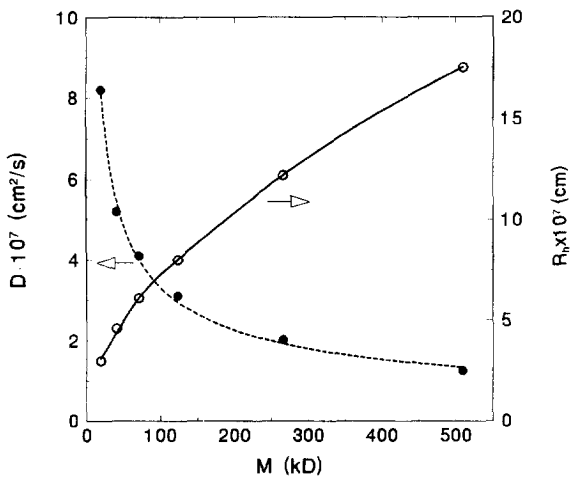

Fig. 1. Diffusion coefficient, D, and hydrodynamics radius, R_h, of dextran molecules as a function of the molecular mass, M.

expressions:

$$D = 2.63 \times 10^{-4} M^{-0.583} \text{ (cm}^2\text{/s) and } R_h = 8.27 \times 10^{-10} M^{-0.583} \text{ (cm)}, \quad (10)$$

where the numerical constants were determined by the least-squares method. A similar expression for $D(M)$ with slightly different numerical constants was reported by Sellen [12].

We measured by SLS the second osmotic virial coefficient, A_2, to check whether specific intermolecular interactions appear between the dextran molecules. The *dimensionless* second virial coefficients [14]:

$$B = \frac{3}{4\pi} A_2 \frac{M^2}{N_A R_h^3} \quad (11)$$

of all investigated samples were close to the theoretical value for particles interacting as hard spheres, $B=4$ [14]. For example, in the case of dextran with $M=40.6$ kD, we measured $A_2 = 5.8 \times 10^{-4}$ cm^3/g^2 mol, $R_h = 4.7$ nm and from Eq. (11) one calculates $B=3.7$, which is very close to the theoretical value for hard spheres. This is an indication that the dextran molecules interact with each other approximately as hard spheres (at least in the absence of shear hydrodynamic fields) with a radius close to that determined by DLS.

3.2. MWCO of unmodified ultrafiltration membranes

First we studied the effects of the applied driving pressure and of the dextran concentration on the measured rejection coefficients of unmodified membranes. The results from these measurements were used to chose the standard conditions for further comparison of the membrane properties before and after modification.

Fig. 2(a) presents the measured rejection coefficients, $Re(M)$ of a polysulphonic membrane at several values of the transmembrane pressure: $\Delta P = 0.5$ bar (curve 1); $\Delta P = 1.0$ bar (curve 2); and $\Delta P = 2$ bar (curve 3). To obtain each of these curves, we separately filtered four commercial dextran fractions. The number of the experimental points on the graph for each curve (7–10 points) is larger because several points can be obtained from one dextran sample containing molecules of different mass (see Section 2.4). Thus, after suitable selection of the used polymer fractions, one can perform the membrane characterization using three or four of the commercial (polydisperse) dextran fractions.

One can see from Fig. 2(a) that the molecular mass which corresponds to 90% rejection (MWCO) is almost the same for curves 1 and 2. The MWCO determined from these data is between 20 and 22 kD, which is very close to the value of 20 kD certified by the membrane manufacturer. Almost 100% rejection is obtained for molecules with molecular mass above 50 kD. The comparison between curves 1, 2 and 3 shows that the increase in the driving pressure up to $\Delta P =$ 2.0 bar leads to a slight shift of the MWCO towards greater values (30 kD).

On the other hand, curve 1 ($\Delta P = 0.5$ bar) exhibits a different shape at the low molecular mass region, compared with curves 2 and 3. In curve 1, the molecular fractions between 3 and 8 kD have almost constant rejection (slightly above 50%). A possible explanation of this experimental fact is that the convective flux is relatively weak, and the backward diffusion flux of the small molecules becomes significant at this low driving pressure. Hence, the small molecules are rejected more efficiently due to their lower concentration in the

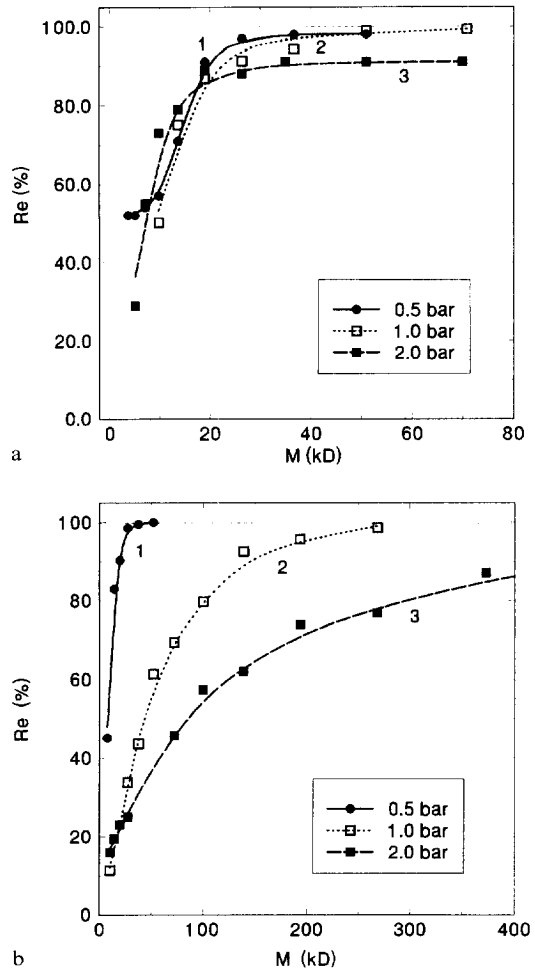

Fig. 2. (a) Influence of the applied transmembrane pressure on the partial rejection coefficient, *Re*, of polysulphonic membrane of certified MWCO = 20 kD: $\Delta P = 0.5$ bar (curve 1); $\Delta P = 1$ bar (curve 2); and $\Delta P = 2$ bar (curve 3). (b) Influence of the applied transmembrane pressure on the partial rejection coefficient, *Re*, of polysulphonic membrane with certified MWCO = 150 kD: $\Delta P = 0.5$ bar (curve 1); $\Delta P = 1$ bar (curve 2); and $\Delta P = 2$ bar (curve 3).

vicinity of the membrane surface. On the contrary, at a higher driving pressure, $\Delta P = 2$ bar, the convective flux is so intensive that even large molecules ($M > 20$ kD) may leak through the membrane yielding $Re = 90\%$ (this effect might be due to deformation of the dextran molecules at these conditions); for 0.5 and 1 bar, the rejection of these large molecules is almost 100%. In conclusion, these results suggest that $\Delta P = 1$ bar is most suitable pressure for membrane characterization, at least in this pore size range.

The influence of the applied driving pressure on the determined MWCO is even more pronounced when a membrane with larger pores is studied. Fig. 2(b) presents results for the ultrafiltration membrane of certified MWCO = 150 kD. Curves 1, 2 and 3 correspond to $\Delta P = 0.5$, 1.0 and 2 bar, respectively. One observes a dramatic change in the $Re(M)$ curves and in the MWCO value with the increase of the applied pressure (similar results were reported in previous studies [6,7]). As explained below, the deposition of latex particles reduced the MWCO of this membrane from 150 to 45 kD. Bearing in mind the results from Fig. 2(a), we chose $\Delta P = 1.0$ bar as a standard driving pressure for the further comparison of the retention characteristics of the membranes before and after coating with latex spheres.

The influence of the *polymer concentration* in the feed solution on the rejection coefficients was checked with the same membrane (MWCO = 150 kD) at $\Delta P = 1.0$ bar within the concentration range between 0.25 and 2 wt.% dextran. The increase in the total polymer concentration above 1 wt.% shifted the MWCO towards smaller values. The explanation of this observation could be the formation of a gel layer (dynamic membrane) at higher total concentrations, which would increase the retention of the small dextran fractions. We did not find any significant differences in the measured MWCO values when using solutions with total dextran concentrations of 0.25 and 0.5 wt.%. For this reason, all other experiments were carried out at 0.5 wt.% because this concentration allows one to perform light scattering and refractometric measurements of the permeates with good accuracy.

3.3. Dependence of the thickness of the deposited layer on the particle charge

The measured ζ potential of the amphoteric latex particles ($d_p = 260$ nm) is presented in Fig. 3(a) as a function of pH. At pH = 8.2, the surface potential is practically zero (isoelectric point, IEP). Below the IEP, the particles are

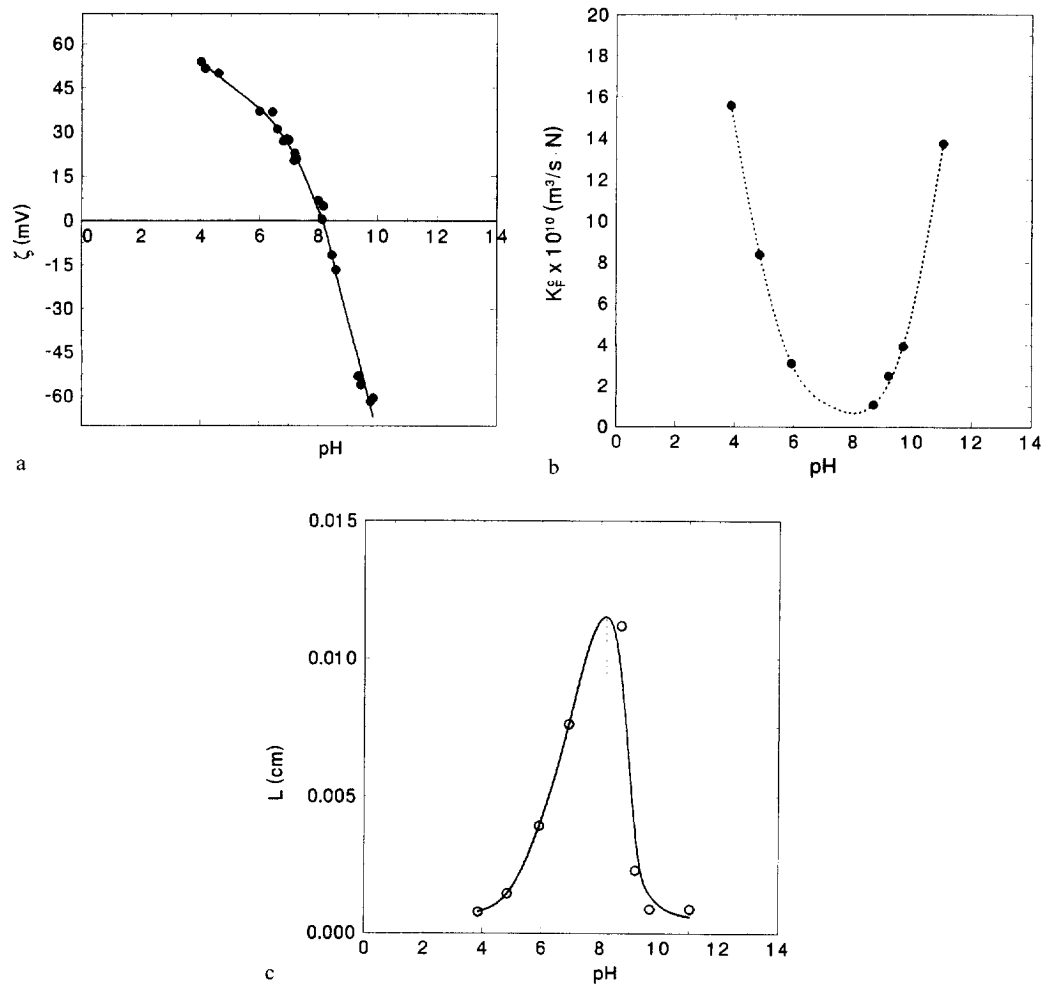

Fig. 3. (a) ζ potential of the amphoteric latex particles ($d_p = 260$ nm) as a function of pH; (b) permeability, K_f^ζ, of the coagulated part of the deposited layer obtained during particle filtration at different pH; (c) thickness, L, of the layer of coagulated latex particles obtained upon filtration at different pH. The circles are experimental results and the curve is a guide for the eye.

positively charged, while above the IEP, they are negatively charged. In both cases, a strong electrostatic repulsion between the particles should appear far from the isoelectric point. On the other hand, the polysulphonic membrane is negatively charged in the entire pH range such that one might expect an electrostatic attraction between the particles and the membrane surface at pH < 8.2.

The filtration experiments carried out with the same particles and with a polysulphonic membrane of MWCO = 150 kD showed that the total membrane permeability (including that of the deposited layer) was strongly influenced by the particle surface potential. In Fig. 3(b), we show the results for the calculated permeability of the *coagulated part* of the cake as a function of pH (for the procedure of determination of K_f^ζ see Section 2.2). The minimum of the permeability is in the vicinity of the isoelectric point of the latex particles [cf. Fig. 3(a)]. This result might be expected because most enhanced coagulation of the particles is expected around the IEP [15]. The permeability of the layer increases with the magnitude of the particles' ζ potentials irrespectively of its sign. This

result can be explained with the formation of a thicker coagulated layer around the IEP. Indeed, the thickness of the coagulated layer, L, determined as explained in Section 2.2, shows a well-pronounced maximum around the IEP — see Fig. 3(c). The layer thickness around the IEP is of the order of 100 μm, which corresponds to several hundreds of particle layers, one over the other.

In conclusion, a coagulated particle deposit is formed around the IEP, and one could expect that the membrane properties are substantially modified at these conditions (see Section 3.4). However, the formation of a very thick coagulated layer results in a strong reduction of the membrane permeability [Fig. 3(b)], which should be avoided. Thus, an optimum layer thickness (depending on the particular system) can be searched for. As seen from Fig. 3(c), the layer thickness can be controlled well by varying pH of the suspension. Other factors which might be used for control of the layer thickness are the particle concentration in the feed suspension and the driving pressure during the layer formation.

3.4. Modified membranes

We tried to modify the membrane with MWCO = 150 kD by filtering polystyrene latex (d_p = 140 nm) with $\zeta = -60$ mV, as well as by filtering PBCA latex (d_p = 107 nm) with $\zeta = -33$ mV. In both cases, the rejection curves $Re(M)$ obtained before and after treating the membrane with these particles were practically the same. These results mean that the electrostatic repulsion between the particles dominates and they cannot coagulate at these "soft" conditions to form a thick enough layer. As shown in Ref. [4], the addition of neutral electrolyte in many cases (e.g. when the particle surface potential is weakly dependent on the electrolyte concentration) would not lead to particle coagulation and the suspension remains stable.

As could be expected, the filtration of particles having a lower surface potential (PBCA latex with $\zeta = -12$ mV) resulted in the formation of a coagulated layer (at the same experimental conditions) and in a substantial change of the membrane retention ability — see Fig. 4. The comparison between curves 1 and 2 in Fig. 4 shows that the formation of deposited layer resulted in the following changes:

(1) the MWCO value decreased from 150 down to 40 kD;
(2) the selectivity of the membrane was improved, which is shown by the much steeper initial slope of curve 2 compared with curve 1.

Therefore, the relatively simple deposition process described above resulted in a substantial change of the membrane retention characteristics. The fact that the rinsing of the membrane with water does not wash the coagulated layer shows that the latter has enough mechanical stability to allow careful handling of the membrane. In principle, the deposited particle layer can be further treated (e.g. by thermal annealing or by adsorption of polymers) in order to increase its stability and to further modify its filtration properties.

As discussed in Section 2.3, the dynamic light scattering allows one to relate the molecular mass of the polymer with the size of the dextran molecules. The inset in Fig. 4 shows the partial rejection coefficient Re as a function of the hydrodynamic radius, R_h. One can see that the modified mem-

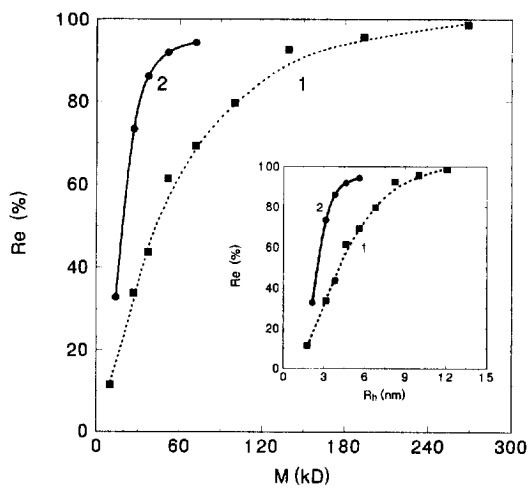

Fig. 4. Partial rejection coefficient $Re(M)$ of polysulphone membrane before (curve 1) and after (curve 2) deposition of layer of PBCN particles ($\zeta = -12$ mV). The inset shows Re as a function of the hydrodynamic radius, R_h, of the dextran molecules: unmodified (curve 1); and modified (curve 2) membrane.

brane rejects (rather well) molecules which are about two times smaller than the nonmodified membrane (cf. curves 1 and 2 in the inset). The MWCO value of the modified membrane corresponds to dextran molecules with $R_h \approx 4.5$ nm. It is worthy to note that this value is about two times smaller compared with the value which is calculated from Eq. (1). Indeed, the diameter of the particles used to form the layer was $d_p = 107$ nm, and Eq. (1) predicts that spherical polymer molecules of radius about 8 nm could pass through the array of particles. This result is easily understood considering the fact that the hydrodynamic radius [defined by the Stokes–Einstein relationship, Eq. (7)] is substantially smaller than the geometrical size of the polymer molecule [16] due to the loose structure of the molecules. The relationship between the hydrodynamic radius, R_h, of a *random coil* and the mean square end-to-end distance, $\langle R^2 \rangle^{1/2}$, of the polymer chain (which is a measure of the molecular size) is [16]:

$$R_h = (3\pi/32)^{1/2} \langle R^2 \rangle^{1/2} \approx 0.54 \langle R^2 \rangle^{1/2}. \quad (12)$$

If we assume that the dextran molecules have the structure of a random coil (which is an approximation), the mean square end-to-end distance of the rejected molecules is $\langle R^2 \rangle^{1/2} \geqslant 8.3$ nm, which is very close to the value predicted by Eq. (1). Therefore, the agreement between the predicted limiting size of the rejected molecules and the experimental results is rather good if we consider the mean square end-to-end distance as a characteristic size of the dextran molecules.

4. Conclusions

The performed experiments show that a coagulated layer of monodisperse latex spheres deposited over the membrane can substantially change the membrane retention characteristics — the molecular weight cut-off value is reduced and the selectivity of the membrane is improved (see Fig. 4). The limiting size (mean square end-to-end distance) of the rejected dextran molecules agrees very well with the calculated radius from the minimal cross-sectional area of the "pore" formed between three neighboring particles, Eq. (1).

The experiments show that at the used relatively low transmembrane pressure ($\Delta P \leqslant 2$ bar), only particles of ζ potential below approximately 30 mV in magnitude form an irreversibly coagulated layer. Otherwise, the particles do not coagulate during the filtration process and redisperse after the filtration is ceased. The thickness of the deposited layer can be controlled by several parameters — pH of the suspension (if amphoteric latex is used), duration of the deposition process, concentration of the particles, etc.

The characterization of the membranes was performed by using the well-known method of filtering polymer molecules (dextrans) of different molecular mass. However, we measured the molecular mass distribution of the polymer in the permeates by using dynamic light scattering (DLS) as an alternative to the commonly used gel-permeation chromatography. In some cases DLS method can be advantageous because: (1) a precise calibration with expensive, perfectly monodisperse samples is not necessary — see the procedure developed in Appendix A; and (2) the hydrodynamic radius of the molecules is directly measured.

Acknowledgment

The authors are indebted to Professor Furusawa (University of Tsukuba, Japan) for the synthesis of the polystyrene latex and to Dr M Simeonova (Institute of Special Polymers, Sofia, Bulgaria) for the synthesis of the polybutylcyanoacrylate latex. This study was supported by the Bulgarian Ministry of Education, Science and Technology.

Appendix A

In this appendix, the procedure for determination of the constants a and b in Eq. (6) is described. The main difficulty arose from the fact that the light scattering experiments were performed with commercial dextran samples with certain size distribution of the molecules within each sample. In a polydisperse polymer sample, the average molecular mass, $\bar{M}$ (which is directly measured in the static light scattering experiments) can be related

to the average diffusion coefficient, $\bar{D}$ (which is determined in the dynamic light scattering experiments) in the following way:

$$\bar{M}=\sum_i P_i M_i=\sum_i P_i a D_i^b=a\bar{D}^b \sum_i P_i\left(1+\frac{\Delta D_i}{\bar{D}}\right)^b$$

$$\approx a\bar{D}^b \sum_i P_i\left(1+bx+\frac{b(b-1)}{2}x^2+\cdots\right), \quad \text{(A1)}$$

where $x_i=(\Delta D_i)/(\bar{D})$. P_i is the molar fraction of the polymer of mass M_i in the sample ($\Sigma P_i=1$, $\Sigma P_i x_i=0$). Hence:

$$\bar{M}\approx a\bar{D}^b\left[1+\frac{b(b-1)}{2}\sigma_D^2\right]. \quad \text{(A2)}$$

$\sigma_D^2=\Sigma_i P_i x_i^2$ is the standard deviation which is measured in the DLS experiments. In our experiments $(\sigma_D^2)^{1/2}$ was between 0.18 and 0.28 for all samples.

Eq. (A2) can be written in the form:

$$\ln\left[\frac{\bar{M}}{1+\frac{b(b-1)}{2}}\sigma_D^2\right]=\ln a+b\ln\bar{D}, \quad \text{(A3)}$$

where $\bar{M}$, $\bar{D}$ and σ_D are known from the experiment for a series of dextran samples, while the parameters a and b have to be calculated. For this purpose, we used an iterative computational procedure based on a counterpart of Eq. (A3):

$$\ln\left[\frac{\bar{M}}{1+\frac{b_n(b_n-1)}{2}}\sigma_D^2\right]=\ln a_{n+1}+b_{n+1}\ln\bar{D}, \quad \text{(A4)}$$

where a_k and b_k are consecutive approximations determined in the iterative procedure.

The following algorithm was used:

(1) Determination of the average molecular mass, $\bar{M}$, by using static light scattering. The value of $\bar{M}$ given by the manufacturer can be used as well.

(2) Measurements of $\bar{D}$ and σ_D by dynamic light scattering.

(3) Plotting $\bar{M}$ versus ln $\bar{D}$ and obtaining the initial values, a_0 and b_0 from the intercept and the slope of the obtained straight line.

(4) Plotting

$$\ln\left[\frac{\bar{M}}{1+\frac{b_0(b_0-1)}{2}\sigma_D^2}\right]$$

versus ln $\bar{D}$ and determining the next values, a_1 and b_1, from the new straight line.

(5) Plotting

$$\ln\left[\frac{\bar{M}}{1+\frac{b_1(b_1-1)}{2}\sigma_D^2}\right]$$

vs ln $\bar{D}$, thus obtaining a_2 and b_2. The procedure can be repeated to obtain more precise values but usually two or three steps provided sufficient accuracy.

(6) Using the final values, $a=7.235\times10^{-7}$ and $b=-1.7152$, we calculate the *molecular mass distribution* in the sample from the *diffusion coefficient distribution* — see Eq. (6).

A plot of the experimental points and the straight line determined by the least squares method is shown in Fig. 5. The correlation coefficient is 0.994.

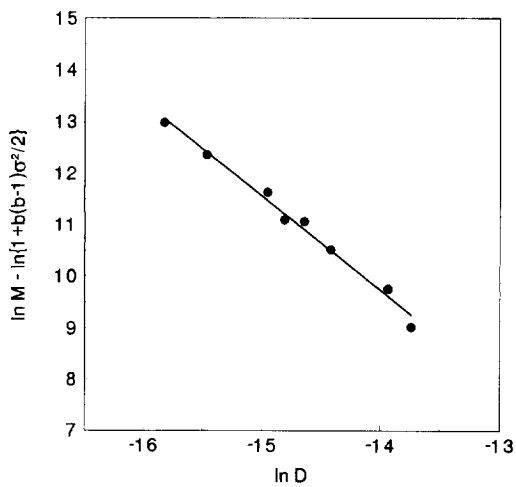

Fig. 5. Calibration line used to determine the constants a and b from the light scattering results (see the Appendix A).

References

[1] T.D. Brok, Membrane Filtration, Science and Technology Institute, Madison, WI, 1983.
[2] M.C. Porter, in: P. Schweitzer (Ed.), Handbook of Separation Techniques for Chemical Engineers, McGraw-Hill, New York, 1988.
[3] W.B. Russel, D.A. Saville, W.R. Schowalter, Colloidal Dispersions, Cambridge University Press, Cambridge, 1989.
[4] D.N. Petsev, V.M. Starov, I.B. Ivanov, Colloids Surf. 81 (1993) 65.
[5] P. Abaticchio, A. Botino, G. Camera Roda, G. Capannelli, S. Minari, Desalination 78 (1990) 235.
[6] G. Schak, A. Miquel, R. Birkenberger, J. Membrane Sci. 41 (1989) 55.
[7] R. Nobrega, H. De Balmann, P. Aimar, V. Sanchez, J. Membrane Sci. 45 (1989) 17.
[8] A. Corona, J.E. Rollings, Sep. Sci. Technol. 23 (1988) 855.
[9] J. Happel, H. Brenner, Low Reynolds Number Hydrodynamics and Application to Particulate Media, Prentice Hall, New York, 1965.
[10] M.B. Huglin (Ed.), Light Scattering from Polymer Solutions, Academic Press, London, 1972.
[11] D.W. Schaefer, C.C. Han, in: R. Pecora (Ed.), Dynamic Light Scattering, Plenum Press, London, 1985.
[12] D.B. Sellen, Polymer 16 (1975) 561.
[13] A. Einstein, Ann. Phys. (Leipzig) 17 (1905) 549.
[14] T.L. Hill, Statistical Thermodynamics, Addison-Wesley, Reading, MA, 1960.
[15] E.J.W. Verwej, J.Th.G. Overbeek, Theory and Stability of Lyophobic Colloids, Elsevier, Amsterdam, 1948.
[16] A.Y. Grosberg, A.R. Hohlov, Statistical Physics of Macromolecules, Nauka, Moscow, 1989 (in Russian).